Medicine®

DIAGNOSTIC ACCURACY STUDY

OPEN

Intratumoral Agreement of High-Resolution Magic Angle Spinning Magnetic Resonance Spectroscopic Profiles in the Metabolic Characterization of Breast Cancer

Vivian Youngjean Park, MD, Dahye Yoon, MS, Ja Seung Koo, MD, PhD, Eun-Kyung Kim, MD, PhD, Seung Il Kim, MD, PhD, Ji Soo Choi, MD, PhD, Seho Park, MD, Hyung Seok Park, MD, Suhkmann Kim, PhD, and Min Jung Kim, MD, PhD

Abstract: High-resolution magic angle spinning (HR-MAS) magnetic resonance (MR) spectroscopy data may serve as a biomarker for breast cancer, with only a small volume of tissue sample required for assessment. However, previous studies utilized only a single tissue sample from each patient. The aim of this study was to investigate whether intratumoral location and biospecimen type affected the metabolic characterization of breast cancer assessed by HR-MAS MR spectroscopy

This prospective study was approved by the institutional review board and informed consent was obtained. Preoperative core-needle biopsies (CNBs), central, and peripheral surgical tumor specimens were prospectively collected under ultrasound (US) guidance in 31 patients with invasive breast cancer. Specimens were assessed with HR-MAS MR spectroscopy. The reliability of metabolite concentrations was evaluated and multivariate analysis was performed according to intratumoral location and biospecimen type.

There was a moderate or higher agreement between the relative concentrations of 94.3% (33 of 35) of metabolites in the center and periphery, 80.0% (28 of 35) of metabolites in the CNB and central surgical specimens, and 82.9% (29 of 35) of metabolites between all 3 specimen types. However, there was no significant agreement between the concentrations of phosphocholine (PC) and phosphoethanolamine (PE) in the center and periphery. The concentrations of several metabolites (adipate, arginine, fumarate, glutamate, PC, and PE) had no significant agreement between the CNB and central surgical specimens.

In conclusion, most HR-MAS MR spectroscopic data do not differ based on intratumoral location or biospecimen type. However, some metabolites may be affected by specimen-related variables, and caution is recommended in decision-making based solely on metabolite concentrations, particularly PC and PE. Further validation through future studies is needed for the clinical implementation of these biomarkers based on data from a single tissue sample.

(*Medicine* 95(15):e3398)

Abbreviations: CNB = core-needle biopsy, ER = estrogen receptor, HER2 = human epidermal growth factor receptor 2, HR-MAS = high-resolution magic angle spinning, ICC = intraclass correlation coefficient, IHC = immunohistochemistry, MR = magnetic resonance, PC = phosphocholine, PE = phosphoethanolamine, PLS-DA = partial least squares discriminant analysis, PR = progesterone receptor, US = ultrasound.

INTRODUCTION

Magnetic resonance (MR) spectroscopy is a promising modality that can quantitatively analyze metabolic alterations in breast cancer and help identify potential targets for personalized therapy.[1] Although in vivo MR spectroscopy can provide information that encompasses the entire tumor lesion, the breast spectra typically can only display a single metabolite peak representing the total choline (tCho).[2] However, recent advances have enabled the detection of various metabolites in breast cancer tissue using high-resolution magic angle spinning (HR-MAS) MR spectroscopy. HR-MAS MR spectroscopy is a nondestructive technique that provides spectra with multiple peaks from intact tissue.[3] Through the discrimination and quantification of choline-containing compounds and various other metabolites, HR-MAS MR spectra provide a vast amount of biological information. Previous studies using HR-MAS MR spectroscopy data have reported that the metabolic profiles of breast cancer specimens differ according to clinicopathologic factors and may serve as a potential marker for tumor aggressiveness.[4–8]

Heterogeneity within individual tumors has been extensively reported in both morphological and genomic studies. Immunomarkers including human epidermal growth factor receptor 2 (HER2) and microRNA expression levels have shown intratumoral heterogeneity in breast cancer, suggesting that testing on more representative larger tumor samples or at

Editor: Wen Zhou.
Received: December 14, 2015; revised and accepted: March 23, 2016.
From the Department of Radiology and Research Institute of Radiological Science (VYP, E-KK, MJK), Severance Hospital, Yonsei University College of Medicine, Seoul; Department of Chemistry and Chemistry Institute for Functional Materials (DY, SK), Pusan National University, Busan; Department of Pathology (JSK), Department of Surgery (SIK, SP, HSP), Severance Hospital, Yonsei University College of Medicine; and Department of Radiology (JSC), Samsung Medical Center, Sungkyunkwan University School of Medicine, Seoul, Republic of Korea.
Correspondence: Min Jung Kim, Department of Radiology, Research Institute of Radiological Science, Yonsei University College of Medicine, 50 Yonsei-ro, Seodaemun-gu, 03722 Seoul, Republic of Korea (e-mail: mines@yuhs.ac).
Suhkmann Kim, Department of Chemistry and Chemistry Institute for Functional Materials, Pusan National University, Geumjeong-gu, 46241 Busan, Republic of Korea (e-mail: suhkmann@pusan.ac.kr).
This study was supported by the Basic Science Research Program of the National Research Foundation of Korea funded by the Ministry of Science, ICT& Future Planning, Republic of Korea (grant 2013R1A1A3013165), a faculty research grant of Yonsei University College of Medicine for 2015 (6-2015-0050) and 2012 (6-2012-0087), and by Research Institute of Radiological Science, Yonsei University College of Medicine.
The authors have no conflicts of interest to disclose.

ISSN: 0025-7974
DOI: 10.1097/MD.0000000000003398

several different tumor locations may be required for accurate assessment.[9–12] In addition, there have been concerns that specimen type (such as in vivo core-needle biopsy [CNB] sampling and ex vivo surgical sampling) may affect biomarkers or metabolic profiling. In a recent study that assessed in vivo CNB biopsies and central and peripheral surgical breast cancer specimens with reverse-phase protein arrays and immunohistochemistry (IHC), 86% of the proteomic biomarkers did not show significant intratumoral heterogeneity, but 37% of the biomarkers differed between the CNB and surgical specimens.[13] As HR-MAS MR spectroscopy requires only a small volume of tissue sample, it is unclear whether these results can be considered to be representative of the entire lesion. In addition, to the best of our knowledge, no studies have directly compared HR-MAS spectroscopy data between CNB and surgical specimens in patients with breast cancer.

Therefore, the purpose of this study was to investigate whether intratumoral location and biospecimen type (in vivo collection of core biopsy samples or ex vivo collection of surgical tumor samples) affect the metabolic characterization of breast cancer as assessed by HR-MAS MR spectroscopy.

MATERIALS AND METHODS

Study Population and Specimen Acquisition

This prospective study was approved by the institutional review board of Yonsei University College of Medicine, and written consent was obtained from each patient. Between July 2014 and January 2015, 71 female patients who fulfilled the following inclusion criteria were initially enrolled: 20 years of age or older, not pregnant at the time of diagnosis, no history of breast cancer, and had either undergone ultrasound (US)-guided CNB at our institution for breast lesions assessed as category 4 or 5 and larger than 1 cm in diameter on US images, or were referred to our hospital after being diagnosed with breast cancer. Nine patients with benign pathology results on CNB and 27 patients from whom surgical tumor samples were not obtainable immediately following surgical removal were excluded. Of the remaining 35 patients, 28 patients underwent US-guided CNB preoperatively at our institution and 7 patients were referred to our hospital after being diagnosed with breast cancer. From the 28 patients who were diagnosed at out institution, 1 CNB specimen was obtained at the time of preoperative US-guided CNB and was included in our study. For all 35 patients, 2 core tissue samples were obtained from the tumor under US guidance following surgical removal. Thus, 98 core tissue samples from 35 patients were initially included in our study – 28 tissue samples obtained preoperatively in 28 patients and 70 tissue samples obtained from surgical specimens from 35 patients.

Our research team was contacted at the beginning of the enrolled patients' surgeries, and a member from the team prepared a portable icebox containing ice blocks and an US unit for biopsy. Following surgical removal of the tumor, the surgical tumor specimens were immediately placed on top of the ice blocks and carried to the US unit. Two tissue samples were obtained under US guidance using a 14-guage dual-action semiautomatic core biopsy needle (Stericut with coaxial guide, TSK Laboratory, Tochigi, Japan), obtained from both the tumor center and periphery. The core tissue sample from the tumor center was obtained by targeting the epicenter of the tumor with a core biopsy needle. In large cancers with solid and cystic components, the homogeneously solid areas were targeted. The core tissue sample from the periphery of the tumor was obtained from within the tumor boundary seen on US. In 1 patient who was diagnosed with breast cancer at our institution, 2 core tissue samples were later obtained from the center of the surgical tumor specimen, as the periphery of the lesion was primarily cystic. For HR-MAS MR spectroscopy, all tissue samples were put in a cryogenic vial and immersed in liquid nitrogen immediately after biopsy. Samples were stored at $-162\,^{\circ}C$ for 1 to 7 months prior to HR-MAS MR spectroscopy. After HR-MAS MR spectroscopy, all 98 tissue samples were assessed by hematoxylin and eosin (H&E) staining and subsequently 7 samples with no tumor cells on H&E staining were excluded. Consequently, 4 patients had only 1 sample and were also excluded from the study. In total, 87 tissue samples from 31 patients (mean age 54.2 years; range 31–75 years) were included, which composed our study population.

HR-MAS MR Spectroscopy

HR-MAS MR spectroscopy was performed on the tumor specimens using a nuclear magnetic resonance (NMR) spectrometer (Agilent, VNMRS 600). The proton NMR frequency was set to 600.17 MHz (11.74 T) and the temperature was set to $26\,^{\circ}C$. After defrost, the tissue samples were weighed and placed in an HR-MAS nanoprobe (Agilent, Walnut Creek, CA), with a total cell volume of 40 μL. Samples weighing an average of 8.19 mg were put in the cell with the remainder filled with D_2O containing 2 mM trimethylsilyl propionic acid (TSP). An inverse-detection type probe with a single Z gradient coil was used. Analysis was performed using a Carr–Purcell–Meiboom–Gill (CPMG) pulse sequence to apply a T2 filter. All spectra were obtained at a spinning rate of 2 kHz. The spectral acquisition parameters were as follows: 16.384 K complex data points, 9615.4 Hz sweep width, 1.704-s acquisition time, 1.0-s relaxation delay, 2.0-s presaturation time, 256 number of transients, and total acquisition time of 16 minutes and 18 seconds. Each spectrum was processed and analyzed using Chenomx NMR suite 7.1 software (Chenomx Inc., Canada). Postprocessing included Fourier transformation, phasing, and baseline correction. Chemical shifts were referenced in relation to the TSP signal at 0.00 ppm. Quantification was performed by comparing the concentration of the metabolites to the concentration of the TSP in each sample cell.

Histopathologic Analysis

All 31 tumors were pathologically diagnosed as malignant based on CNB prior to surgery. The final histopathologic results after surgery were used as reference standards. Pathological data including histologic tumor size, nuclear grade, histologic grade, and lymph node metastasis were obtained from the final pathologic reports. All samples were fixed in 10% buffered formalin and paraffin. The hematoxylin and eosin (H&E)-stained slides for each case were analyzed by experienced pathologists. The histologic grade of each tumor was determined with the modified Bloom–Richardson classification.[14] Information on the expression status of the estrogen receptor (ER), progesterone receptor (PR), HER2, and Ki-67 status were obtained from the CNB specimens. IHC analyses for ER, PR, HER2, and Ki-67 were performed using tissue blocks. ER and PR positivity were defined as the presence of at least 10% positive tumor nuclei in the sample on testing.[15] The IHC staining results for HER2 were scored as 0, 1+, 2+, or 3+ according to the number of cells stained positively on the membrane. Tumors with a score of 3+ were classified as HER2-positive, and tumors with scores of 0 or 1+ were

classified as HER2-negative. Gene amplification using fluorescence in situ hybridization was performed in tumors with a score of 2+ to determine HER2 status.[16,17] Triple negative breast cancer was defined as a tumor negative for ER, PR, and HER2. The IHC staining results for Ki-67 were scored according to the number of cells with positively stained nuclei and were expressed as percentages of the total tumor cells. Staining results for Ki-67 were classified as low $<14\%$ and high $\geq 14\%$.[18]

Statistical Analysis

The reliability of HR-MAS MR spectroscopic values of the metabolite concentrations (acetate, adipate, alanine [Ala], arginine [Arg], asparagine [Asn], aspartate [Asp], betaine, choline [Cho], creatine [Cr], ethanolamine, fumarate, glucose, glutamate [Glu], glutamine [Gln], glycerol, glycine [Gly], glycerophosphcholine [GPC], histidine [His], isoleucine [Ile], lactate, leucine [Leu], lysine [Lys], methionine [Met], phosphocholine [PC], phosphoethanolamine [PE], phenylalanine [Phe], proline [Pro], serine [Ser], taurine, total choline [tCho, the sum of Cho, PC, and GPC], threonine [Thr], tyrosine [Tyr], uracil, valine [Val], and myo-inositol [m-Ins]) among all 3 specimen types (CNB samples collected in vivo vs central surgical tumor samples collected ex vivo vs peripheral surgical tumor samples collected ex vivo) was assessed using the intraclass correlation coefficient (ICC). Post hoc analysis between the following groups were performed using ICCs with Bonferroni correction: CNB samples collected in vivo versus central surgical tumor samples collected ex vivo, and central surgical tumor samples collected ex vivo versus peripheral surgical tumor samples collected ex vivo. ICC values that did not include 0 in their respective 95% confidence intervals were considered to show statistically significant agreement. ICC values in the following ranges were considered to indicate poor (0–0.2), fair (0.21–0.4), moderate (0.41–0.60), substantial (0.61–0.80), or almost perfect agreement (0.81–1.00).[19] Differences in HR-MAS MR spectroscopic values according to intratumoral location and biospecimen type were analyzed using the paired t test between CNB samples versus central surgical samples and between central surgical samples versus peripheral surgical samples. Statistical analysis was conducted using statistical software (version 20.0; SPSS, Chicago, IL). A 2-tailed *P* value less than 0.05 indicated a statistically significant difference.

To evaluate whether specimen type affected the metabolic profiling of breast cancer based on multivariate data analysis, we performed multivariate analysis of the spectral data using Matlab (MathWorks, Natick, MA), SIMCA-P 12.0 (Umetrics, Sweden), and Excel (Microsoft, Seattle, WA) programs. Multivariate partial least squares discriminant analysis (PLS-DA) was performed to evaluate whether different specimen types had similar performance in distinguishing patient groups by hormone receptor status (ER, PR, and HER2), for which previous studies have reported clear separation using multivariate models.[4,5,7] To avoid over-fitting of the statistical model, class discrimination models were built until cross-validated predictability values did not increase significantly. Signals contributing to class discrimination were identified by an S-plot, with identification of the corresponding HR-MAS MR spectral data using Chenomx (Spectral database; Edmonton, Alberta, Canada) software and an in-house database.

RESULTS

The mean tumor size of the 31 malignant breast lesions was 21.8 mm (range, 11–46 mm). The most common tumor type was invasive ductal carcinoma (n = 28) and other cancer types were 2 mixed invasive ductal carcinoma and invasive lobular carcinoma, and 1 mixed mucinous carcinoma and invasive micropapillary carcinoma. The clinicopathologic data of the 31 malignant breast lesions from the 31 patients are presented in Table 1.

Of the 35 metabolites, 94.3% (33 of 35) showed a moderate or higher level of agreement between the central and peripheral surgical specimens (Table 2). Substantial to almost perfect agreement was seen in 60.0% of the metabolites (21 of 35). However, PC (ICC 0.194, 95% CI, −0.173–0.514) and PE (ICC 0.241, 95% CI, −0.125–0.549) did not show significant agreement between the tumor center and periphery.

Between CNB and central surgical specimens, 82.9% (29 of 35) of the metabolites showed significant agreement, with 80.0% (28 of 35) showing a moderate or higher level of agreement. Among all 3 specimen types, all of the metabolites showed a fair or higher level of agreement, with 82.9% (29 of 35) showing a moderate or higher level of agreement (Figures 1 and 2). The 17.1% (6 of 35) of metabolites showing fair agreement among all 3 specimen types also showed fair or no significant agreement between the central and peripheral surgical specimens or between the CNB and central surgical specimens. Using the paired t test, most of the metabolites showed no significant difference between the central and peripheral surgical specimens (97.1%, 34 of 35) and between the CNB and central surgical specimens (94.3%, 33 of 35) (Table 3).

TABLE 1. Clinicopathologic Characteristics of the 31 Patients With Invasive Breast Cancers

Clinicopathologic Variables		Patients, %
Age (mean ± SD)	Years	54.2 ± 12.8
Histologic grade	Low	14 (45.2)
	High	17 (54.8)
Nuclear grade	Low	17 (54.8)
	High	14 (45.2)
ER status	Negative	10 (32.3)
	Positive	21 (67.7)
PR status	Negative	20 (64.5)
	Positive	11 (35.5)
HER2 status	Negative	23 (74.2)
	Positive	8 (25.8)
Triple negativity	Negative	26 (83.9)
	Positive	5 (16.1)
Ki-67 status	Low	11 (35.5)
	High	20 (64.5)
Immunohistochemistry subtype	Luminal A	9 (29.0)
	Luminal B	8 (25.8)
	Luminal-HER2	4 (12.9)
	HER2 enriched	5 (16.1)
	Triple negative	5 (16.1)
Tumor size (mean ± SD)	mm	22.0 ± 9.7
Lymph node metastasis	Negative	20 (64.5)
	Positive	11 (35.5)

Continuous variables (age, tumor size) are presented as mean ± standard deviation. ER = estrogen receptor, HER2 = human epidermal growth factor receptor 2, PR = progesterone receptor, SD = standard deviation.

TABLE 2. Reliability of HR-MAS MR Spectroscopic Values Among Specimen Types

Metabolite	Scenter Vs Speriphery ICC (95% CI)	CNB Vs Scenter ICC (95% CI)	All Specimen Types ICC (95% CI)
Acetate	0.456 (0.121, 0.698)	0.688 (0.409, 0.850)	0.622 (0.402, 0.797)
Adipate	0.731 (0.507, 0.862)	0.197 (−0.207, 0.544)	0.307 (0.057, 0.572)
Alanine	0.533 (0.220, 0.747)	0.392 (0.005, 0.677)	0.355 (0.057, 0.572)
Arginine	0.614 (0.331, 0.796)	0.380 (−0.009, 0.670)	0.390 (0.138, 0.637)
Asparagine	0.742 (0.525, 0.868)	0.709 (0.443, 0.861)	0.540 (0.301, 0.744)
Aspartate	0.676 (0.423, 0.832)	0.551 (0.207, 0.774)	0.483 (0.237, 0.705)
Betaine	0.626 (0.348, 0.803)	0.463 (0.091, 0.722)	0.579 (0.348, 0.770)
Cho	0.667 (0.409, 0.827)	0.810 (0.616, 0.912)	0.461 (0.212, 0.690)
Creatine	0.526 (0.210, 0.742)	0.741 (0.494, 0.877)	0.652 (0.440, 0.815)
Ethanolamine	0.791 (0.606, 0.895)	0.754 (0.518, 0.884)	0.633 (0.415, 0.803)
Fumarate	0.601 (0.312, 0.788)	0.348 (−0.046, 0.649)	0.291 (0.043, 0.559)
Glucose	0.523 (0.206, 0.741)	0.639 (0.333, 0.823)	0.556 (0.321, 0.755)
Glutamate	0.597 (0.307,0.785)	0.376 (−0.014, 0.667)	0.422 (0.171, 0.661)
Glutamine	0.512 (0.154, 0.751)	0.525 (0.172, 0.759)	0.599 (0.377, 0.779)
Glycerol	0.577 (0.279, 0.773)	0.619 (0.304, 0.812)	0.613 (0.390. 0.791)
Glycine	0.698 (0.455, 0.844)	0.553 (0.209, 0.775)	0.574 (0.342, 0.766)
GPC	0.729 (0.504, 0.861)	0.703 (0.433, 0.857)	0.786 (0.630, 0.893)
Histidine	0.733 (0.512, 0.864)	0.547 (0.201, 0.771)	0.434 (0.183, 0.670)
Isoleucine	0.672 (0.417, 0.829)	0.559 (0.218, 0.778)	0.547 (0.310, 0.749)
Lactate	0.561 (0.257, 0.764)	0.642 (0.338, 0.825)	0.404 (0.152, 0.648)
Leucine	0.721 (0.491, 0.857)	0.667 (0.377, 0.838)	0.487 (0.241, 0.708)
Lysine	0.702 (0.462, 0.846)	0.740 (0.494, 0.877)	0.619 (0.398, 0.795)
Methionine	0.697 (0.454, 0.843)	0.568 (0.230, 0.783)	0.473 (0.225, 0.698)
PC	0.194 (−0.173, 0.514)	0.268 (−0.134, 0.594)	0.391 (0.139, 0.639)
PE	0.241 (−0.125, 0.549)	0.218 (−0.186, 0.559)	0.248 (0.003, 0.523)
Phenylalanine	0.735 (0.514, 0.864)	0.760 (0.528, 0.887)	0.640 (0.425, 0.808)
Proline	0.489 (0.155, 0.722)	0.631 (0.313, 0.821)	0.408 (0.151, 0.656)
Serine	0.550 (0.242, 0.757)	0.427 (0.046, 0.699)	0.454 (0.205, 0.685)
Taurine	0.611 (0.327, 0.794)	0.495 (0.132, 0.741)	0.520 (0.278, 0.731)
tCho	0.530 (0.215, 0.745)	0.498 (0.136, 0.743)	0.448 (0.199, 0.681)
Threonine	0.563 (0.260, 0.765)	0.630 (0.320, 0.818)	0.515 (0.273, 0.728)
Tyrosine	0.712 (0.478, 0.852)	0.700 (0.427, 0.855)	0.574 (0.341, 0.766)
Uracil	0.560 (0.256, 0.763)	0.716 (0.455, 0.864)	0.531 (0.291, 0.738)
Valine	0.713 (0.480, 0.853)	0.629 (0.318, 0.817)	0.546 (0.309, 0.748)
m-Ins	0.632 (0.358, 0.806)	0.545 (0.199, 0.770)	0.636 (0.419, 0.806)

All specimen types include CNB specimens, central surgical specimens, and peripheral surgical specimens. Cho = choline, CI = confidence interval, CNB = core-needle biopsy, GPC = glycerophosphocholine, HR-MAS = high-resolution magic angle spinning, ICC = intraclass correlation coefficient, m-Ins = myo-inositol, MR = magnetic resonance, PC = phosphocholine, PE = phosphoethanolamine, Scenter = central surgical specimen, Speriphery = peripheral surgical specimen, tCho = total choline (the sum of Cho, PC, and GPC).

For multivariate analysis, PLS-DA models were produced separately for each specimen type (in vivo CNB specimens, central surgical specimens, and peripheral surgical specimens). In all 3 specimen types, PLS-DA models exhibited the highest sensitivity for discriminating HER2-positive tumors from HER2-negative tumors, with a range of 75.0% to 80.0% (Table 4, Figure 3). Corresponding PLS-DA loading plots showed that PC and glycine were contributing metabolites for the discrimination between HER2-positive and HER2-negative tumors. Based on the PLS-DA loading plots, PC, glycine, and Cho were the contributing metabolites for the discrimination between PR-positive and PR-negative tumors (data not shown). In all 3 specimen types, PLS-DA showed the lowest sensitivity and the highest specificity in discriminating ER-positive tumors from ER-negative tumors, with a range of 47.1% to 66.7% and 62.5% to 90.0%, respectively. Corresponding PLS-DA loading plots showed that PC and glycine were the contributing metabolites in the discrimination of tumors according to ER status (data not shown).

DISCUSSION

To support prognostication and personalized treatment strategies based on the results from a single tumor biopsy sample, it is critical to investigate the possible influences from specimen-related variables on HR-MAS MR spectroscopy data. In our study, most of the HR-MAS MR spectroscopic values showed moderate to substantial agreement between the tumor center and periphery (94.3%) and between the CNB and central surgical specimens (82.9%). Our study results suggest that overall, intratumoral location and biospecimen type have a limited influence on HR-MAS MR spectroscopy data in breast cancer and thus, interpretation based on a single tissue sample is feasible for most metabolites.

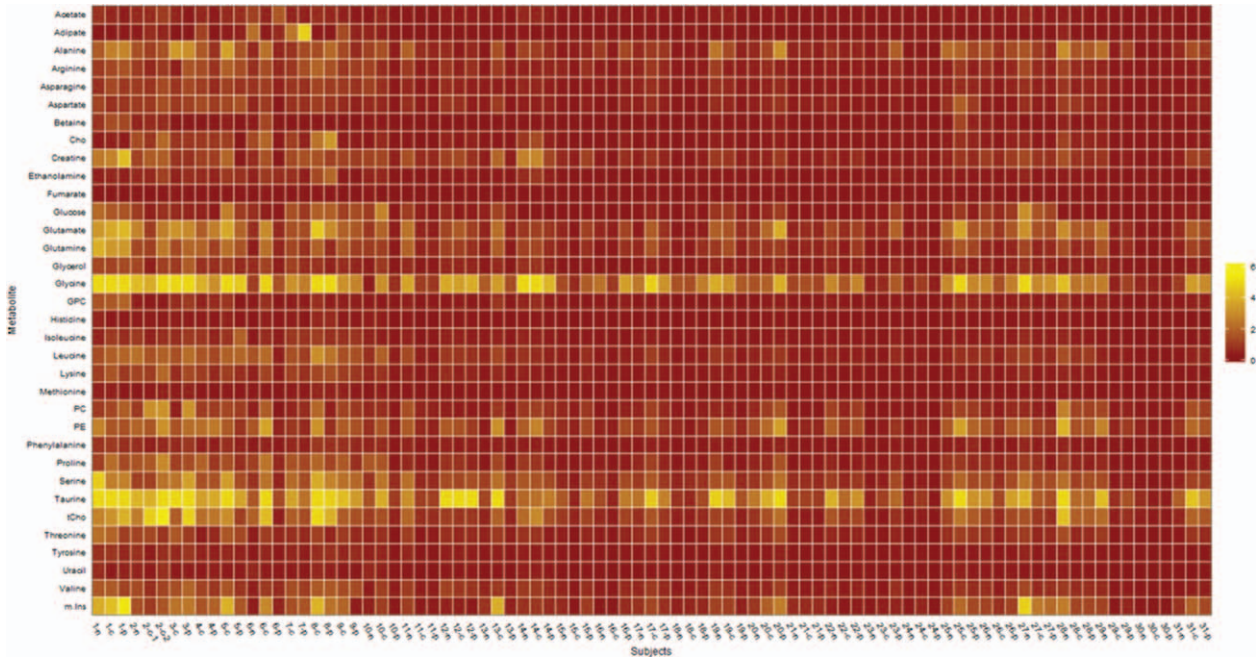

FIGURE 1. Heatmap showing metabolite concentrations for each tissue sample. Each column represents 1 tissue sample and each row represents a different metabolite. ''-n,'' core needle biopsy specimen; ''-c,'' central surgical specimen; ''-p,'' peripheral surgical specimen. Lactate is not shown because a much wider scale range would be required to express its higher range of values (maximum value: 70), and would obscure differences in other metabolite concentrations between samples.

However, concentrations of PC and PE were most affected by specimen type and did not agree between the tumor center and periphery or between CNB and central surgical specimens. In in vivo ^{31}P MR spectroscopy, PC and PE constitute a mixed phosphomonoester (PME) signal that has been shown to be elevated in many types of cancer cells and to correlate with treatment outcome.[20] A recent study on ^{31}P HR-MAS MR spectroscopy found that PE levels were significantly decreased

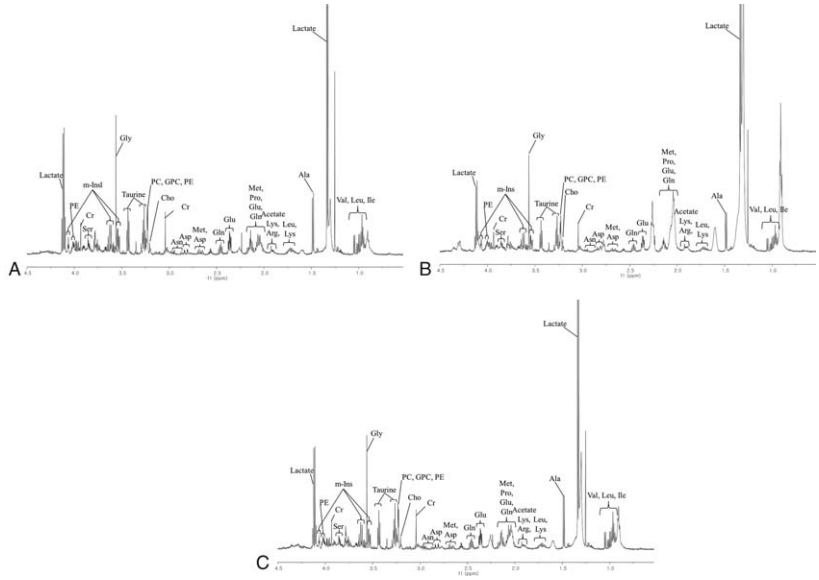

FIGURE 2. HR-MAS MR spectra of breast cancer tissue obtained from a 42-year-old woman with invasive ductal carcinoma (ER-negative, PR-negative, HER2-positive, and tumor size 1.9 cm). PC, Cho, and GPC levels by relative quantification were 0.10, 0.03, and 0.16 for the CNB specimen, 0.12, 0.05, and 0.10 for the central surgical specimen, and 0.06, 0.03, and 0.11 for the periphery surgical specimen, respectively. (A) HR-MAS MR spectra of the CNB specimen, (B) the central surgical specimen, and (C) the peripheral surgical specimen, all obtained from the primary breast cancer. Cho = choline, CNB = core-needle biopsy, ER = estrogen receptor, GPC = glycerophosphcholine, HER2 = human epidermal growth factor receptor 2, HR-MAS = high-resolution magic angle spinning, MR = magnetic resonance, PC = phosphocholine, PR = progesterone receptor.

TABLE 3. Difference of HR-MAS MR Spectroscopic Values Between Specimen Types

				P Value	
Metabolite	**CNB**	**Central**	**Peripheral**	**Scenter Vs Speriphery**	**CNB Vs Scenter**
Acetate	0.248 ± 0.251	0.297 ± 0.230	0.241 ± 0.294	0.765	0.380
Adipate	0.191 ± 0.444	0.277 ± 0.490	0.263 ± 0.865	0.848	0.288
Alanine	1.022 ± 0.818	1.137 ± 0.876	1.002 ± 0.849	0.415	0.583
Arginine	0.530 ± 0.358	0.597 ± 0.477	0.585 ± 0.427	0.820	0.443
Asparagine	0.437 ± 0.274	0.519 ± 0.359	0.428 ± 0.265	0.166	0.413
Aspartate	0.463 ± 0.290	0.591 ± 0.433	0.457 ± 0.332	0.086	0.773
Betaine	0.158 ± 0.181	0.265 ± 0.409	0.131 ± 0.227	0.132	0.247
Cho	0.345 ± 0.373	0.556 ± 0.619	0.362 ± 0.594	0.198	0.577
Creatine	0.786 ± 0.684	0.969 ± 0.734	0.722 ± 0.767	0.155	0.444
Ethanolamine	0.217 ± 0.168	0.359 ± 0.331	0.288 ± 0.370	0.462	0.255
Fumarate	0.072 ± 0.048	0.088 ± 0.068	0.066 ± 0.043	0.051	0.776
Glucose	0.056 ± 0.702	0.705 ± 0.708	0.509 ± 0.480	0.084	0.920
Glutamate	1.241 ± 1.033	1.605 ± 1.195	1.331 ± 1.069	0.149	0.671
Glutamine	1.237 ± 0.892	1.048 ± 0.816	0.847 ± 0.781	0.703	0.009
Glycerol	0.391 ± 0.329	0.504 ± 0.355	0.390 ± 0.351	0.153	0.950
Glycine	2.586 ± 1.820	3.156 ± 2.161	2.845 ± 1.918	0.349	0.825
GPC	0.293 ± 0.298	0.336 ± 0.318	0.291 ± 0.359	0.227	0.831
Histidine	0.155 ± 0.123	0.185 ± 0.133	0.149 ± 0.114	0.081	0.416
Isoleucine	0.283 ± 0.196	0.376 ± 0.271	0.360 ± 0.360	0.976	0.711
Lactate	9.838 ± 6.977	12.067 ± 11.159	12.498 ± 14.962	0.422	0.492
Leucine	0.653 ± 0.533	0.904 ± 0.737	0.727 ± 0.630	0.187	0.905
Lysine	0.334 ± 0.267	0.558 ± 0.502	0.397 ± 0.320	0.172	0.278
Methionine	0.124 ± 0.088	0.201 ± 0.253	0.133 ± 0.090	0.233	0.741
PC	0.603 ± 0.566	0.840 ± 0.781	0.651 ± 0.646	0.788	0.506
PE	1.324 ± 0.956	1.489 ± 1.012	1.079 ± 0.748	0.080	0.836
Phenylalanine	0.262 ± 0.190	0.369 ± 0.342	0.283 ± 0.192	0.291	0.691
Proline	0.582 ± 0.434	0.901 ± 0.778	0.521 ± 0.407	0.011	0.329
Serine	1.142 ± 0.967	1.389 ± 0.961	1.204 ± 0.789	0.210	0.945
Taurine	2.744 ± 1.917	3.437 ± 0.961	2.810 ± 2.039	0.091	0.534
tCho	1.241 ± 1.004	1.707 ± 1.431	1.304 ± 1.175	0.338	0.539
Threonine	0.627 ± 0.482	0.677 ± 0.493	0.529 ± 0.309	0.092	0.506
Tyrosine	0.258 ± 0.183	0.311 ± 0.200	0.272 ± 0.178	0.458	0.655
Uracil	0.206 ± 0.175	0.208 ± 0.188	0.168 ± 0.118	0.876	0.040
Valine	0.589 ± 0.408	0.725 ± 0.478	0.656 ± 0.414	0.359	0.652
m-Ins	1.015 ± 1.139	1.402 ± 1.269	1.067 ± 1.099	0.050	0.450

Data are shown as mean ± standard deviation. Cho = choline, CNB = core-needle biopsy, GPC = glycerophosphocholine, HR-MAS = high-resolution magic angle spinning, ICC = intraclass correlation coefficient, m-Ins = myo-inositol, MR = magnetic resonance, PC = phosphocholine, PE = phosphoethanolamine, Scenter = central surgical specimen, Speriphery = peripheral surgical specimen, tCho = total choline (the sum of Cho, PC, and GPC).

TABLE 4. Diagnostic Performance of PLS-DA for Differentiating Hormone Receptor Status According to Specimen Type

	Specimen Type	**ER^{pos} Vs ER^{neg}, %**	**PR^{pos} Vs PR^{neg}, %**	**$HER2^{pos}$ Vs $HER2^{neg}$, %**
CNB	Sensitivity	47.1	90.0	80.0
	Specificity	62.5	66.7	55.0
Scenter	Sensitivity	66.7	72.7	75.0
	Specificity	90.0	75.0	60.9
Speriphery	Sensitivity	55.0	60.0	75.0
	Specificity	80.0	60.0	54.5

CNB = core-needle biopsy, ER^{neg} = ER negative, ER^{pos} = ER positive, $HER2^{neg}$ = HER2 negative, $HER2^{pos}$ = HER2 positive, PLS-DA = partial least squares discriminant analysis, PR^{neg} = PR negative, PR^{pos} = PR positive, Scenter = central surgical specimen, Speriphery = peripheral surgical specimen.

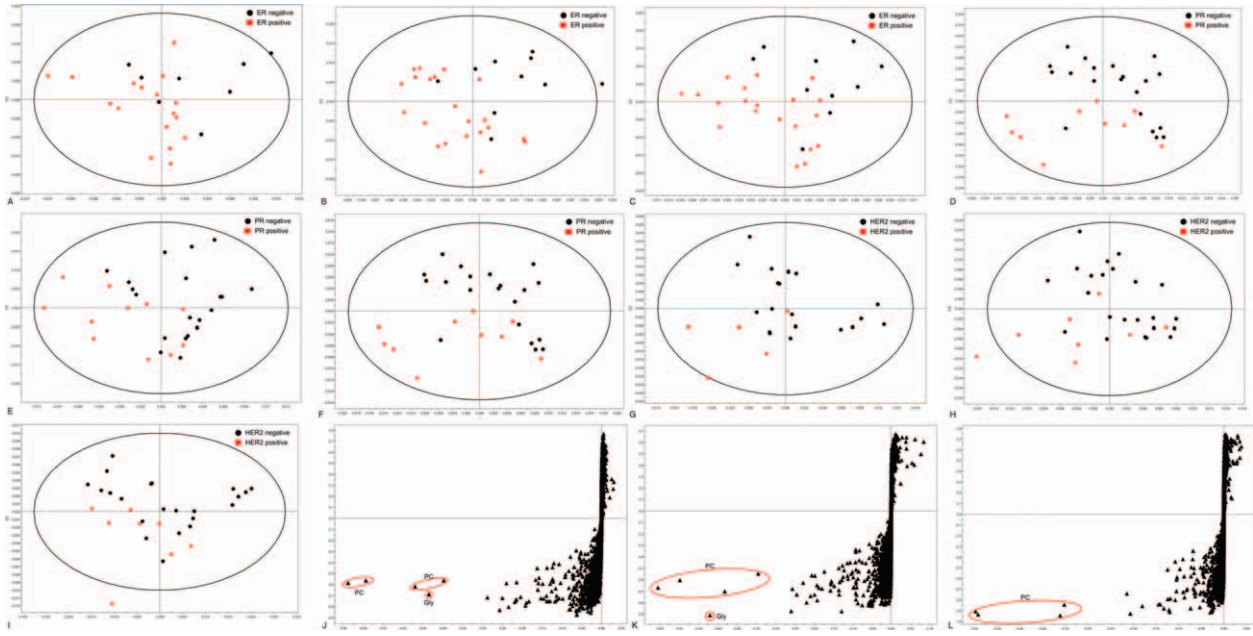

FIGURE 3. PLS-DA score plots of the HR-MAS MR spectra for ER, PR, HER2 status, and loading plots of HER2-positive versus HER-negative breast cancers according to each specimen type. (A–C) PLS-DA score plot for ER status obtained from (A) CNB samples, (B) central surgical samples, and (C) peripheral surgical samples. (D–F) PLS-DA score plot for PR status obtained from (D) CNB samples, (E) central surgical samples, and (F) peripheral surgical samples. (G–I) PLS-DA score plot for HER2 status obtained from (G) CNB samples, (H) central surgical samples, and (I) peripheral surgical samples. (J–L) Loading S-plots of the HR-MAS MR spectra for the discrimination of HER2-positive versus HER2-negative breast cancers in (J) CNB samples, (K) central surgical samples, and (L) peripheral surgical samples. CNB = core-needle biopsy, ER = estrogen receptor, HER2 = human epidermal growth factor receptor 2, HR-MAS = high-resolution magic angle spinning, MR = magnetic resonance, PLS-DA = partial least squares discriminant analysis, PR = progesterone receptor.

in basal-like xenografts after the administration of P13K/mTOR inhibitor BEZ235, whereas PC and GPC levels were increased.[21] As the P13K pathway is a major target for anticancer drug development, our results may imply that sampling from several different tumor locations may be necessary when monitoring treatment response based on ^{31}P MR spectroscopy.[22] In ^{1}H MR spectroscopy, the elevation of PC and tCho levels has also been widely established as a characteristic of cancer cells. The increased tCho levels detected in vivo are primarily due to an increase in PC levels, with a GPC to PC switch having been reported as an early phenotypic change in breast tumor cell lines during carcinogenesis.[23,24] Previous research has shown that the treatment of cancer cells with P13K inhibitors induces a decrease in PC and tCho levels detected by ^{1}H MR spectroscopy, and that a strong correlation is found between PC concentrations and choline kinase α expression.[22] Based on this accumulating research, investigators have suggested the potential role of MR spectroscopy as a noninvasive biomarker for P13K inhibition and tumor response in clinical trials using P13K inhibitors.[22,25] Our results imply that further validation is needed prior to the application of MR spectroscopy for this purpose, as PC measurements from a single tissue sample may not be reliable. In contrast, Cho and GPC levels had moderate to almost perfect agreement, and thus appear to be less affected by intratumoral location and biospecimen type.

Multivariate analysis is commonly used for the interpretation of HR-MAS MR spectral data and can identify trends and clusters related to the sample properties based on the combined influence of metabolites.[26] Recent studies have shown that multivariate models can separate breast cancer samples by hormone receptor status (ER, PR, HER2, and triple negativity) and according to pathologic response to neoadjuvant chemotherapy.[4,5,27] In our study, PLS-DA models showed similar patterns regardless of specimen type, demonstrating the highest sensitivity in discriminating HER2-positive tumors from HER2-negative tumors and the lowest sensitivity in separating ER-positive and ER-negative tumors. The corresponding loading plots demonstrated similar contributing metabolites to the results of Cao et al,[4] with elevated glycine levels in ER-negative, PR-negative, and HER2-positive tumors. Our study results imply that multivariate analysis of HR-MAS MR spectroscopic profiles showed similar results regardless of intratumoral location and biospecimen type, and, thus, can be readily applied in the metabolic characterization of breast cancer biopsy samples.

Our study had several limitations. First, because of its prospective design, our study included a small number of patients and information on long-term follow-up was not available. Therefore, we could not evaluate correlations between HR-MAS MR spectroscopy data and overall or disease-free survival. We believe that an interesting future topic would be establishing the prognostic value of HR-MAS MR spectroscopy in patients with breast cancer. Second, in vivo CNB samples were not available or excluded due to a lack of tumor cells in approximately 25.7% of the patients and could have affected our analysis according to specimen types, especially the analysis between all 3 specimen types. Third, we compared HR-MAS MR spectroscopic values between different portions of a mass, and not among individual cancer cells. This may

partly explain the high overall level of intratumoral agreement in our results; however, the aim of our study was to investigate the influence of specimen-related variables on the metabolic assessment of breast cancer based on a single tissue sample, not at the cellular level, to facilitate its clinical implementation.

In summary, this study demonstrated that overall, intratumoral location and biospecimen type, have limited influence on HR-MAS MR spectroscopic profiles in the metabolic characterization of breast cancer. However, some metabolites are differentially expressed across different specimen types and caution is recommended in clinical decision-making based solely on metabolite concentrations, especially of PC and PE. With further validation by larger studies, ^{1}H HR-MAS MR spectroscopy can be implemented in order to personalize treatment based on data from a single tissue sample.

ACKNOWLEDGMENTS

The authors thank the Basic Science Research Program of the National Research Foundation of Korea funded by the Ministry of Science, ICT& Future Planning, Republic of Korea, faculty research grant of Yonsei University College of Medicine for 2015 (6-2015-0050) and 2012 (6-2012-0087), and Research Institute of Radiological Science, Yonsei University College of Medicine for the support.

REFERENCES

1. Denkert C, Bucher E, Hilvo M, et al. Metabolomics of human breast cancer: new approaches for tumor typing and biomarker discovery. *Genome Med.* 2012;4:37.
2. Bolan PJ. Magnetic resonance spectroscopy of the breast: current status. *Magn Reson Imaging Clin N Am.* 2013;21:625–639.
3. Moestue S, Sitter B, Bathen TF, et al. HR MAS MR spectroscopy in metabolic characterization of cancer. *Curr Top Med Chem.* 2011;11:2–26.
4. Cao MD, Lamichhane S, Lundgren S, et al. Metabolic characterization of triple negative breast cancer. *BMC Cancer.* 2014;14:941.
5. Choi JS, Baek HM, Kim S, et al. HR-MAS MR spectroscopy of breast cancer tissue obtained with core needle biopsy: correlation with prognostic factors. *PLoS One.* 2012;7:e51712.
6. Giskeodegard GF, Grinde MT, Sitter B, et al. Multivariate modeling and prediction of breast cancer prognostic factors using MR metabolomics. *J Proteome Res.* 2010;9:972–979.
7. Li M, Song Y, Cho N, et al. An HR-MAS MR metabolomics study on breast tissues obtained with core needle biopsy. *PLoS One.* 2011;6:e25563.
8. Sitter B, Bathen TF, Singstad TE, et al. Quantification of metabolites in breast cancer patients with different clinical prognosis using HR MAS MR spectroscopy. *NMR Biomed.* 2010;23:424–431.
9. Malinowsky K, Raychaudhuri M, Buchner T, et al. Common protein biomarkers assessed by reverse phase protein arrays show considerable intratumoral heterogeneity in breast cancer tissues. *PLoS One.* 2012;7:e40285.
10. Nassar A, Radhakrishnan A, Cabrero IA, et al. Intratumoral heterogeneity of immunohistochemical marker expression in breast carcinoma: a tissue microarray-based study. *Appl Immunohistochem Mol Morphol.* 2010;18:433–441.
11. Raychaudhuri M, Schuster T, Buchner T, et al. Intratumoral heterogeneity of microRNA expression in breast cancer. *J Mol Diagn.* 2012;14:376–384.
12. Seol H, Lee HJ, Choi Y, et al. Intratumoral heterogeneity of HER2 gene amplification in breast cancer: its clinicopathological significance. *Mod Pathol.* 2012;25:938–948.
13. Meric-Bernstam F, Akcakanat A, Chen H, et al. Influence of biospecimen variables on proteomic biomarkers in breast cancer. *Clin Cancer Res.* 2014;20:3870–3883.
14. Elston CW, Ellis IO. Pathological prognostic factors in breast cancer. I. The value of histological grade in breast cancer: experience from a large study with long-term follow-up. *Histopathology.* 1991;19:403–410.
15. Hammond ME, Hayes DF, Dowsett M, et al. American Society of Clinical Oncology/College of American Pathologists guideline recommendations for immunohistochemical testing of estrogen and progesterone receptors in breast cancer. *J Clin Oncol.* 2010;28:2784–2795.
16. Dolan M, Snover D. Comparison of immunohistochemical and fluorescence in situ hybridization assessment of HER-2 status in routine practice. *Am J Clin Pathol.* 2005;123:766–770.
17. Wolff AC, Hammond ME, Schwartz JN, et al. American Society of Clinical Oncology/College of American Pathologists guideline recommendations for human epidermal growth factor receptor 2 testing in breast cancer. *J Clin Oncol.* 2007;25:118–145.
18. Voduc KD, Cheang MC, Tyldesley S, et al. Breast cancer subtypes and the risk of local and regional relapse. *J Clin Oncol.* 2010;28:1684–1691.
19. Landis JR, Koch GG. The measurement of observer agreement for categorical data. *Biometrics.* 1977;33:159–174.
20. Glunde K, Jiang L, Moestue SA, et al. MRS and MRSI guidance in molecular medicine: targeting and monitoring of choline and glucose metabolism in cancer. *NMR Biomed.* 2011;24:673–690.
21. Esmaeili M, Bathen TF, Engebraten O, et al. Quantitative (31)P HR-MAS MR spectroscopy for detection of response to PI3K/mTOR inhibition in breast cancer xenografts. *Magn Reson Med.* 2014;71:1973–1981.
22. Al-Saffar NM, Jackson LE, Raynaud FI, et al. The phosphoinositide 3-kinase inhibitor PI-103 downregulates choline kinase alpha leading to phosphocholine and total choline decrease detected by magnetic resonance spectroscopy. *Cancer Res.* 2010;70:5507–5517.
23. Aboagye EO, Bhujwalla ZM. Malignant transformation alters membrane choline phospholipid metabolism of human mammary epithelial cells. *Cancer Res.* 1999;59:80–84.
24. Ackerstaff E, Glunde K, Bhujwalla ZM. Choline phospholipid metabolism: a target in cancer cells? *J Cell Biochem.* 2003;90:525–533.
25. Beloueche-Babari M, Jackson LE, Al-Saffar NM, et al. Identification of magnetic resonance detectable metabolic changes associated with inhibition of phosphoinositide 3-kinase signaling in human breast cancer cells. *Mol Cancer Ther.* 2006;5:187–196.
26. Sitter B, Sonnewald U, Spraul M, et al. High-resolution magic angle spinning MRS of breast cancer tissue. *NMR Biomed.* 2002;15:327–337.
27. Choi JS, Baek HM, Kim S, et al. Magnetic resonance metabolic profiling of breast cancer tissue obtained with core needle biopsy for predicting pathologic response to neoadjuvant chemotherapy. *PLoS One.* 2013;8:e83866.